

ACCEPTED MANUSCRIPT



Title: Experimental and Numerical Failure Analysis of a Rotary Vacuum Disc Lime Filter - Part 1: Fluid Flow Study of Filtration Process

Authors: Waldemar F. Cieslakiewicz, Daniel M. Madyira, Marcos Roberto Rodrigues, Wilfrid Grimm, Dewald Scholtz

To appear in: Technical Sciences

Received 28 October 2023;

Accepted 17 July 2024;

Available online 19 July 2024.

This is a PDF file of an unedited manuscript that has been accepted for publication. As a service to our customers we are providing this early version of the manuscript. The manuscript will undergo copyediting, typesetting, and review of the resulting proof before it is published in its final form. Please note that during the production process errors may be discovered which could affect the content, and all legal disclaimers that apply to the journal pertain.

Experimental and Numerical Failure Analysis of a Rotary Vacuum Disc Lime Filter - Part 1: Fluid Flow Study of Filtration Process

Waldemar F. Cieslakiewicz^{1*}, Daniel M. Madyira¹, Marcos Roberto Rodrigues², Wilfrid Grimm², Dewald Scholtz²

¹Department of Mechanical Engineering Science, University of Johannesburg, South Africa

²Drytech International (Pty) Ltd, Johannesburg, South Africa

Corresponding author: waldemarc@uj.ac.za

Abstract

The mechanical separation of solids from liquids (filtration) is a critical process in many chemical process industries. The rotary drum filter can be considered a work-horse device which is one of the oldest filtration devices that has been used for centuries. Its reliability is affected by several process parameters resulting in reduced life and poor separation effectiveness. Common problems include breakage of the filtration medium, wear of filtration holes and breakage of the backing plates. In this work a study is conducted to understand the causes of significant wear exhibited in a single rotary disc vacuum filter to understand the process parameters that led to this failure. The process parameters were recorded and used to validate a CFD model, which in turn was utilised to conduct a parametric study of the systems. The whole study comprises two parts. The first one presents the numerical and experimental analysis of the fluid (water and slurry) flow in the filter, the second one focuses on the numerical and experimental mechanical evaluation of drum filter membrane material.

Keywords

Disc vacuum filter, Cake formation, Cake washing, Cake drying, Cake discharge, Disc wear

Introduction

Rotary drum filters are the work-horse devices for solid-liquid separation in a variety of chemical processes [1]. This applies to the process in which either the solid or the liquid is the required product from a given slurry. Typical application includes the separation of lime from slurry [2]. It generally involves cake formation, washing, drying and discharge depending on the quality of the product required and whether the product is a solid or a liquid. This is realised either through a rotating cylinder or rotating disc [3] configuration. Figure 1(a) and (b) show the configuration of the disc and drum configurations respectively.

In the rotary vacuum disc filter configuration, shown in Figure 2, the disc comprises a number of sectors of stainless steel covered with a fabric filter membrane [4]. The sectors forming a disc are mounted on a hollow shaft that transmits vacuum to the sectors. With a number of discs mounted on a single shaft, the rotary disc vacuum filter provides a much larger filtration area compared to the rotary drum vacuum filter for the same footprint. As the sector dips into the slurry, the vacuum ensures the formation of the filter cake on the filter membrane, which then is carried by the backing plate. As the shaft slowly rotates, the cake is lifted from the slurry, still under vacuum, to allow the cake to dry. To discharge the filter cake, a low pressure burst of air is supplied to the sector to inflate

the membrane and facilitate the scrapping of the cake from the membrane before the sector submerges in the slurry again. This ensures a continuous operation for the process [5].

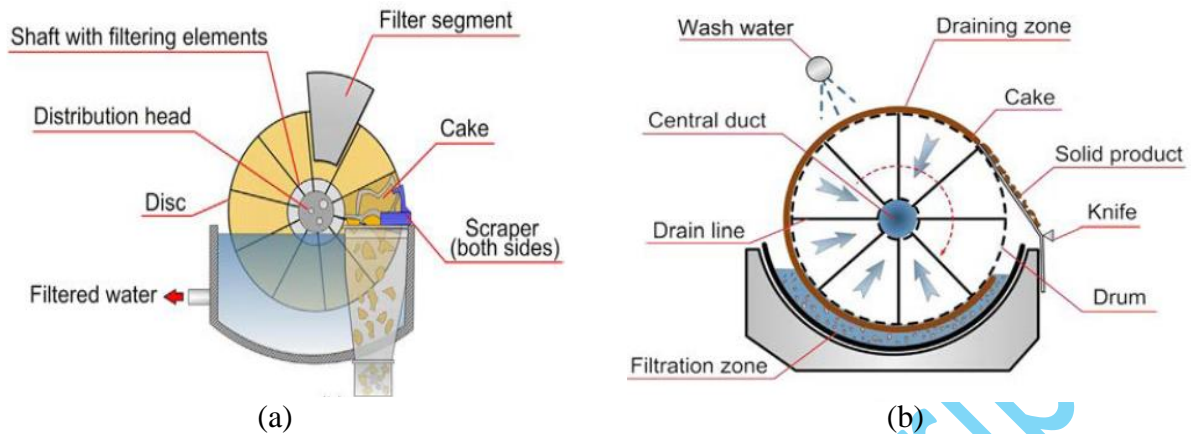


Figure 1: Operating schematic of (a) Rotary disc vacuum filter (b) Rotary drum vacuum filter [4]

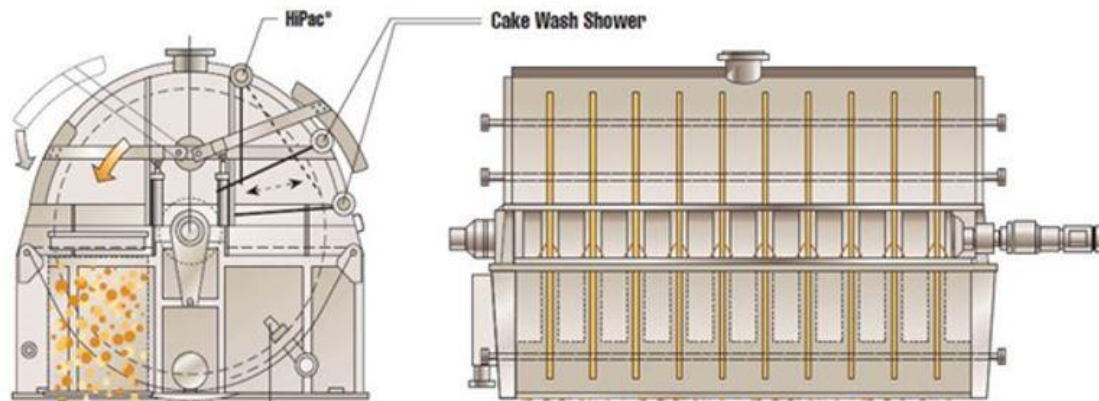


Figure 2: Rotary vacuum disc filter

The performance of the rotary vacuum disk filter can be assessed based on either the effectiveness and efficiency of separation, and the reliability and durability of the filtration equipment. The effectiveness and efficiency of the separation is governed by factors such as particle size, particle shape, particle density, particle size distribution, concentration of particle in the slurry, fluid density, fluid viscosity, fluid temperature, separation membrane parameters (material properties and fabric design), magnitude of vacuum, disc rotational speed etc. [1]. If not properly optimised, some of these factors will also negatively impact on the reliability and durability of the filtering equipment.

This work focused on investigating the parameters that exhibited a significant impact on the high failure rate observed on an existing rotary vacuum disc filter. There is a need to determine the process parameters that resulted in the accelerated failure of the sector backing plate and filter membrane.

System Description

The rotary vacuum disc filtering system under investigation had sectors made of stainless steel wrapped in polypropylene filtration fabric. The system was used to filter lime slurry, which was composed of mainly of dolomite and limestone. The average particle size was 100 μm (98%). Both the backing plate and the filtration membrane had suffered severe damage as shown in Figure 3.



Figure 3: (a) Backing plates sector covered with a filtration membrane. (b) Failure condition of fabric, (Drytech Int.)

The severity of the damage to the backing sector plate is shown in Figure 4. This is characterised by significant erosion which is indicative of elevated particle velocity.



Figure 4: Damage to the sector backing plate, (Drytech Int.)

The filtration disc consists of an assembly of 24 sectors. The material damages pattern was recorded and mapped out in Figure 5. This illustrates that the highest number of material failure was found at the top of each sector (outlet).



Figure 5: Location of material destruction in different disc's sectors, (Drytech Int.)

The performance parameters of the system were recorded for the duration of 1 month of operation time. They are shown in Figure 6. The slurry pump operated at 140 m³/h at a pressure of 4.5 bar and temperature of 85°C. The slurry had a viscosity of 1.57 mm²/s. The re-circulation pump delivered 150m³/h at 6.5 bar and the washing pump 237 m³/h at 1 bar with water at a temperature of 60°C. The precoat renew system operated at 15 bar at 60°C. The precoat was renewed when the discharge cake moisture was above 25% or when the residual alkali in the mud was over 0.21 %.

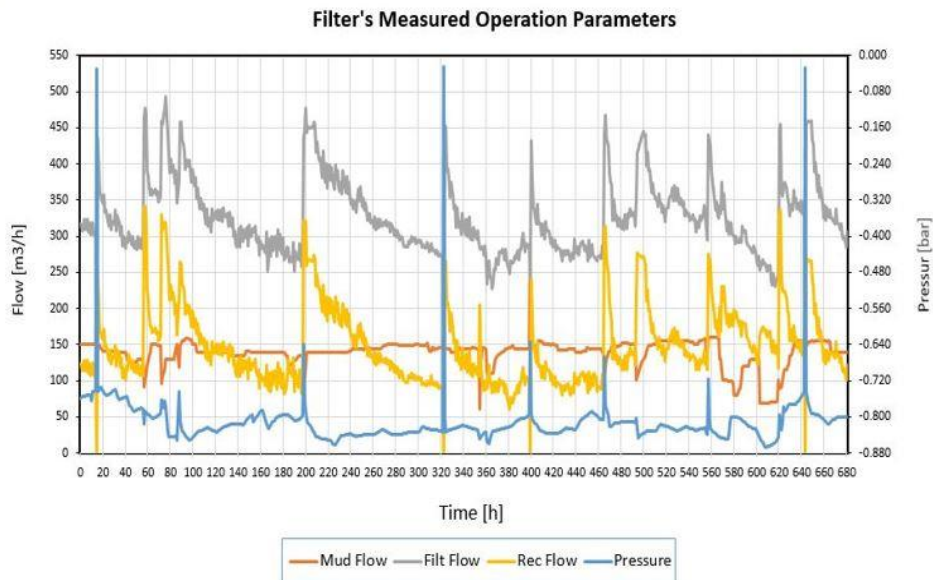


Figure 6: Operating parameters of the system, (Drytech Int.)

In summary, the average flow parameters are as follows: lime slurry flow rate of 139.31 m³/h, filtrate flow rate of 352.98 m³/h, recirculation flow rate of 147.99 m³/h and washing water flow rate of 65.98 m³/h identified as (filtrate flow rate - (slurry flow rate + recirculation flow rate)).

In addition, the graph depicts the pressure characteristic, which is negatively related to the flow rate, that is: the pressure drops, when the filtrate flow increases (shown on the graph). This process is periodical and contingent on the formation of the slurry cake and its removal from the filtration membrane. Further analysis shows that the filtrate flow rate is the key parameter as it's value, the highest velocity of flow, consequently might be the cause of filtration material damage. Furthermore, the operating philosophy, shown in Figure 7, dictates that during periods of low production (<75% of capacity), filtrate from the vacuum receiver needs to be circulated to the feed header to maintain the minimum feed velocity required to maintain agitation levels.

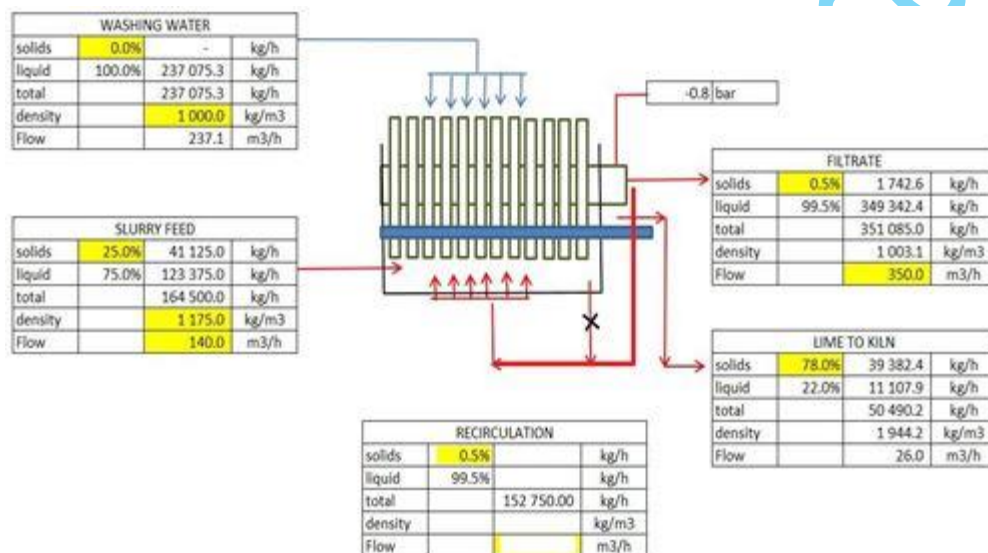


Figure 7: Operating process diagram, (Drytech Int.)

Experiment for Testing Composition (Membrane and Back Perforated Plate) Pressure Drop

The numerical modelling of the system to study the critical flow parameters in the system requires knowledge of the pressure drop and velocity across the filtration membrane. A special test rig was designed and built by Drytech Int. to test the flow behaviour across the membrane. The developed system is shown in Figure 8. The perforated backing plate, shown in Figure 9, was made from stainless steel with 4mm diameter perforations which were spaced 6 mm apart in line with the rotary vacuum disc filter dimensions. The test rig's pressure-measuring chamber has a diameter 155mm, which results in a cross-section area of 0.0188m².

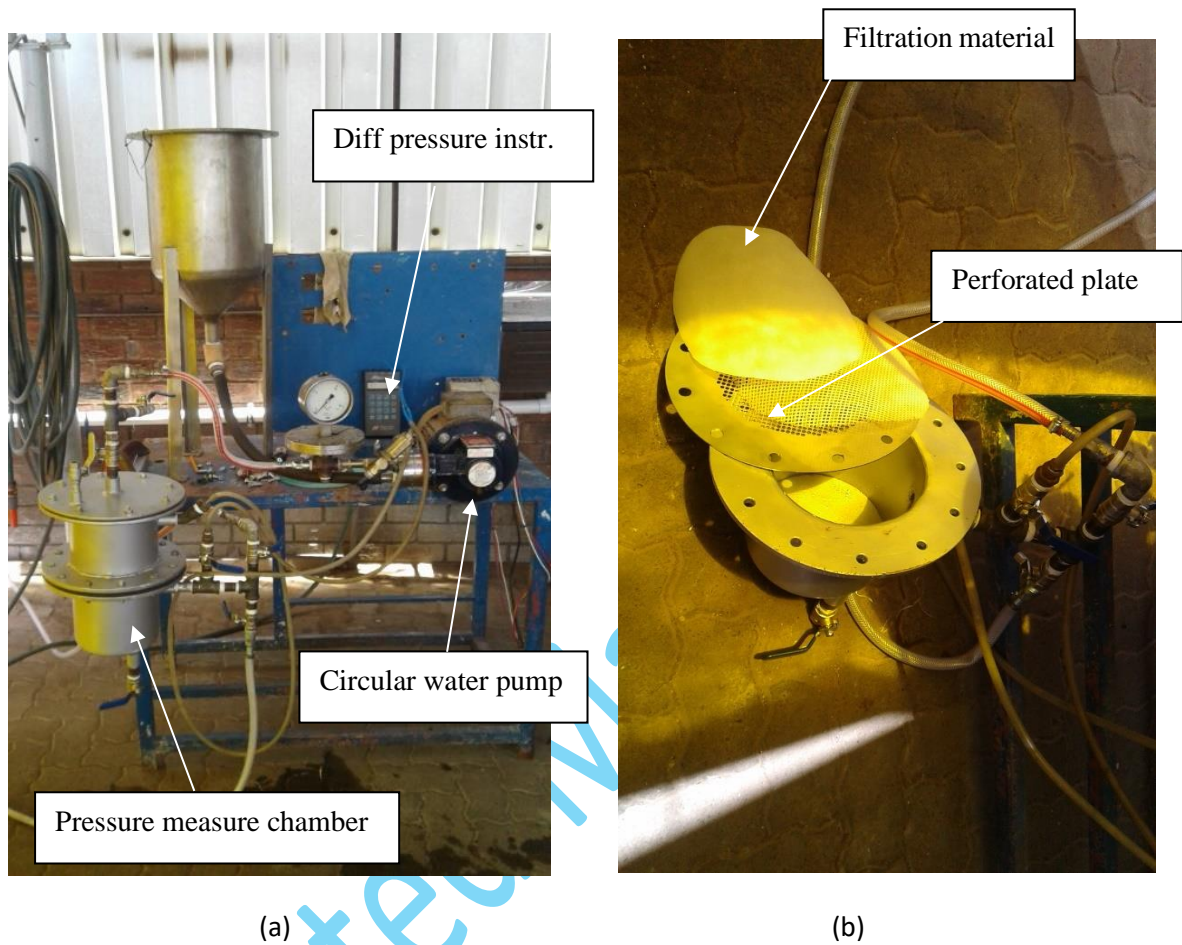


Figure 8: Test rig to measure membrane flow parameters: (a) Set-up, (b) Key components, (Drytech Int.)



Figure 9: Manufactured stainless-steel perforated backing plate, (Drytech Int.)

The pressure drop testing was conducted for flow rates ranging from 0.015 to 0.031 kg/s. This was guided by the operating parameters of the filter. The lowest filter flow rate of 250 m³/h corresponds to 0.017kg/s flow in the test rig. The maximum lime filter flow of 450m³/h stays for 0.031kg/s of mass flow in the test rig, $0.031 = \frac{450 \cdot 1000 \cdot 0.0188}{3600 \cdot 74} \text{ kg/s}$. The calculated superficial water velocity for the maximum lime filter flow of 450m³/h is $0.00168 = \frac{0.031}{1000 \cdot 0.0188} \text{ m/s}$.

Further investigation of the graph in Figure 6 revealed that the highest flow takes place when the suction pressure is at its lowest. At the filter the highest flow 450 m³/h shows the suction pressure to be approximately 0.08bar = 8 kPa. The test rig corresponding flow 0.031 kg/s has a pressure of 6.0 kPa = 0.06bar, illustrated in Figure 10. The suction pressure at the filter has the same value as pressure at the test rig, only sign “-” is used. This pressure difference (8kPa and 6kPa) can be explained by filter’s membrane lower porosity (existence of mud in membrane pores) in comparison to membrane porosity used in test rig.

The pressure drop Δp across the membrane is guided by the formula, Equation 1:

$$\Delta p = \rho(\beta|v_n| + \alpha)v_n \quad \text{eq. 1}$$

where: Δp pressure drop (Pa), v_n is the superficial velocity (m/s), α and β are the user-specified coefficients, and ρ is the fluid density (kg/m³).

The measured data in test rig, shown in Figure 10, were fitted into the first order polynomial ($\beta=0$), $\Delta p = \rho \alpha v_n = \gamma = 2545.7v + 1.8 = \Delta p = 1000\alpha v_n / 1000 + 1.8 \text{ kPa}$. In the model calculation the porous baffle’s (composition) viscous coefficient $\alpha = P_v$ has a value of 2545.7. This value is used in the final model.

The variation of pressure resistance across the composition was measured to be approximately 1.8kPa and max pressure drop was 5.8 kPa, as presented in Figure 10. That pressure is dependent on the flow velocity. The tests were conducted at ambient temperature 24°C and pressure 85kPa. Pressure gauges, shown in Figure 5, were used to measure the pressure drop across the membrane over this range of flow rates, from 0.15 to 0.031 kg/s.

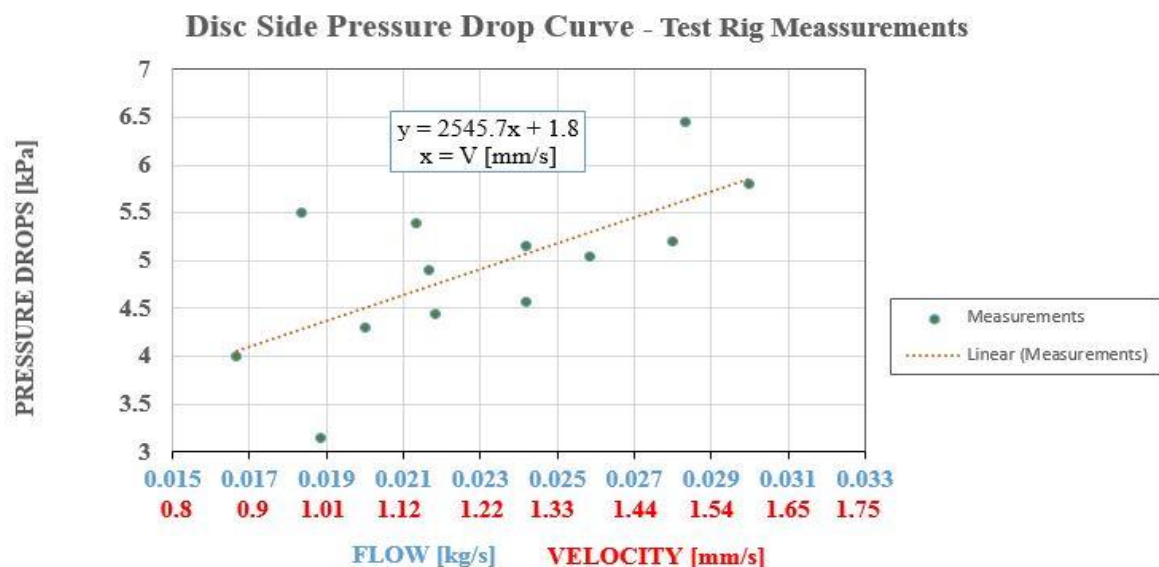


Figure 10: Test rig measured variation of pressure drop across the composition

Model Validation with Experimental Data

To validate the model by data obtained from the measurements, a CFD test rig model was developed. The simulation results are depicted in Figure 11, Figure 12 and Figure 13.

The calculated maximal pressure drop of the filtration membrane on the CFD model is approximately $4.37+1.8=6.17\text{kPa}$, which in comparison to the measured value on the test rig 6.0kPa , at the flow 0.031 kg/s , see Figure 10, is satisfactory. This value reaffirms the previously calculated P_v coefficient, which is then used in the final CFD analysis. The average velocity of 0.006 m/s (6mm/s) at the membrane calculated in the model is presented in Figure 12. These velocities are higher than the experimental superficial velocities. However, they are "inside" membrane velocities, where the cross area of the flow is lower due to its porosity.

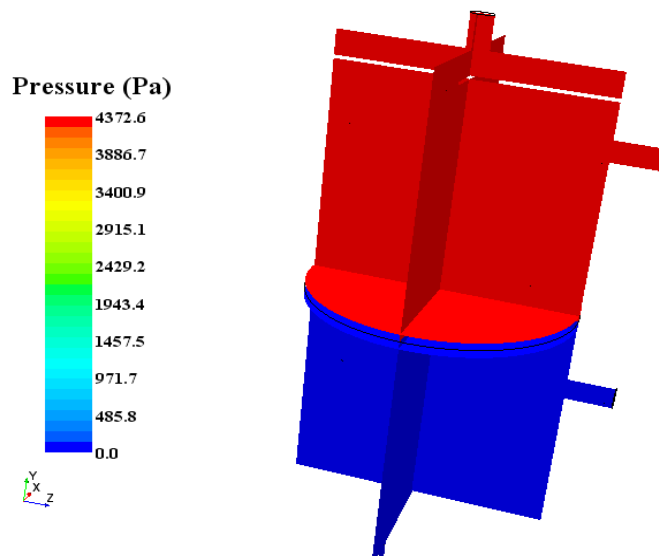


Figure 11: Simulation of pressure distribution in test rig

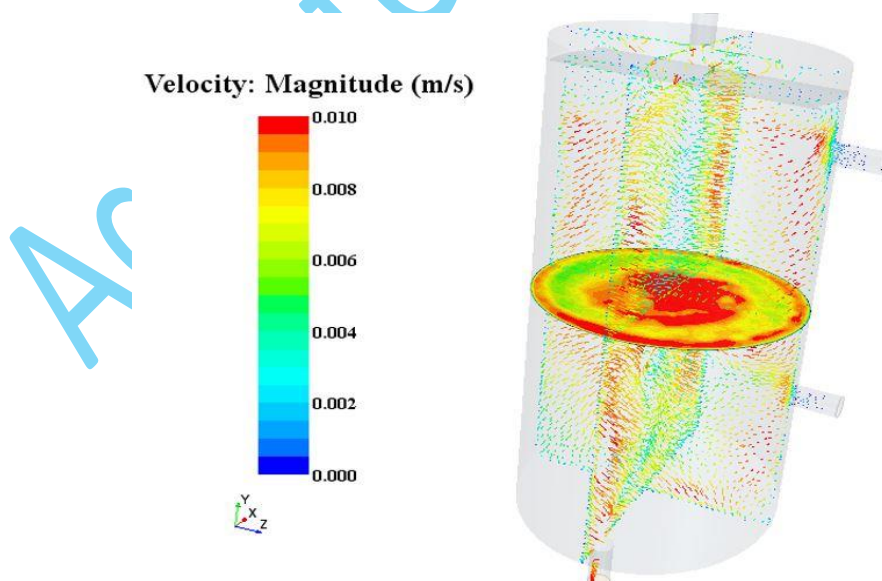


Figure 12: Simulation of velocity distribution through the composition in test rig

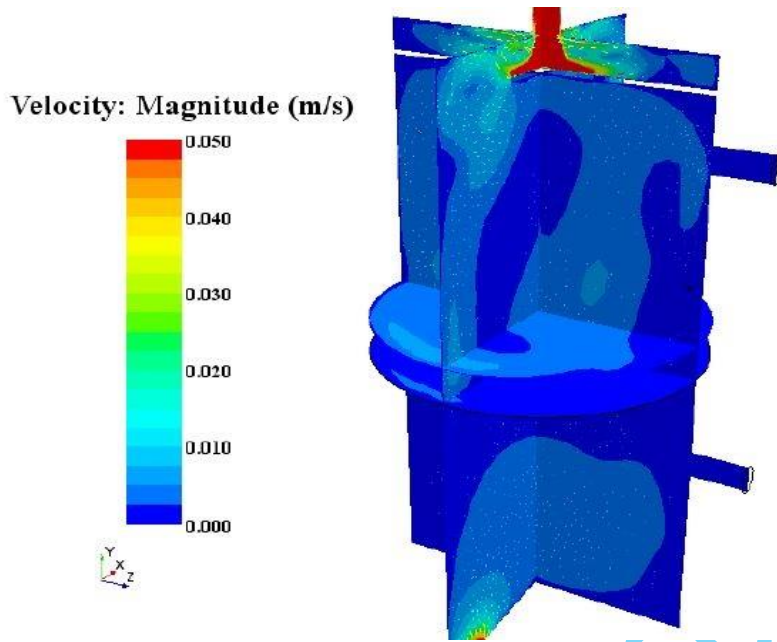


Figure 13: Simulation of velocity magnitude distribution in test rig

Filtrate Cake Pressure Drop Experiment

Lime mud cake properties were investigated experimentally. The test rig was designed and built by Drytech Int., see Figure 14. The lime mud cake was measured at a thickness 0.023m of a porous material. The pressure drop across the lime filter cake was determined experimentally.

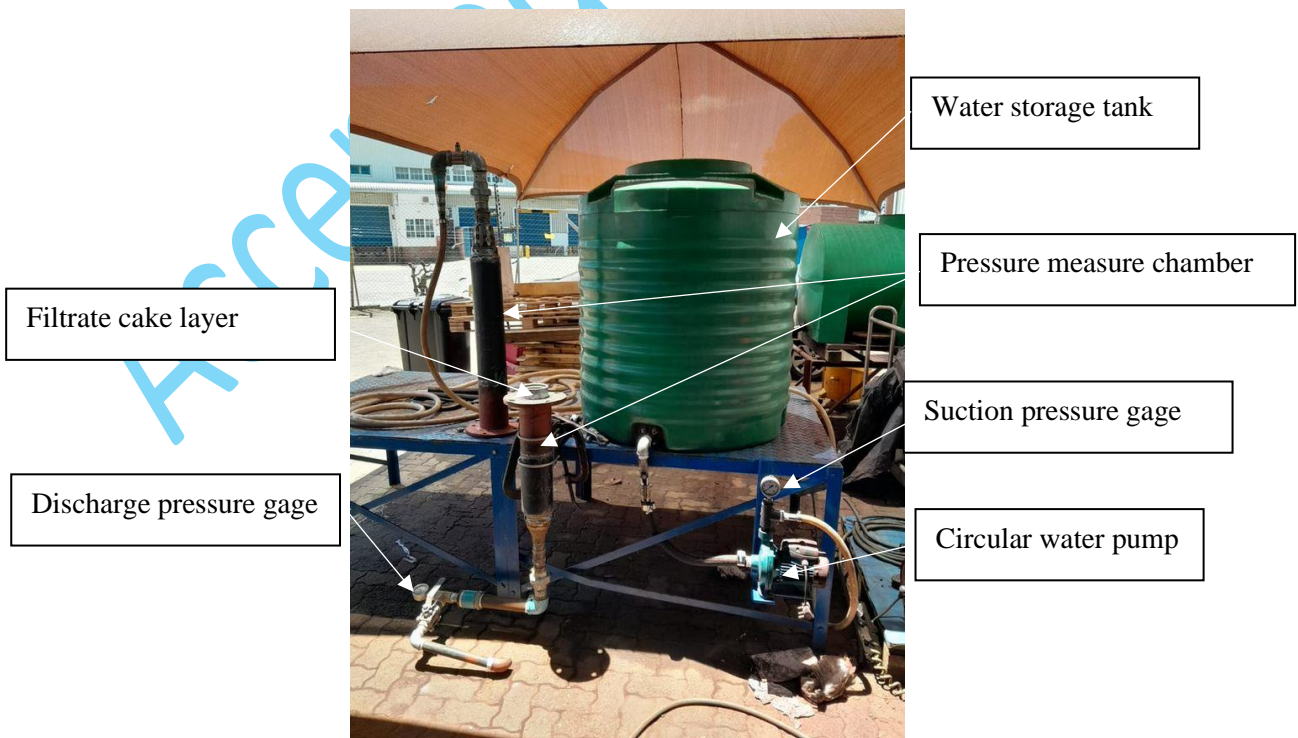


Figure 14: Test rig to measure filtration cake flow parameters, (Drytech Int.)

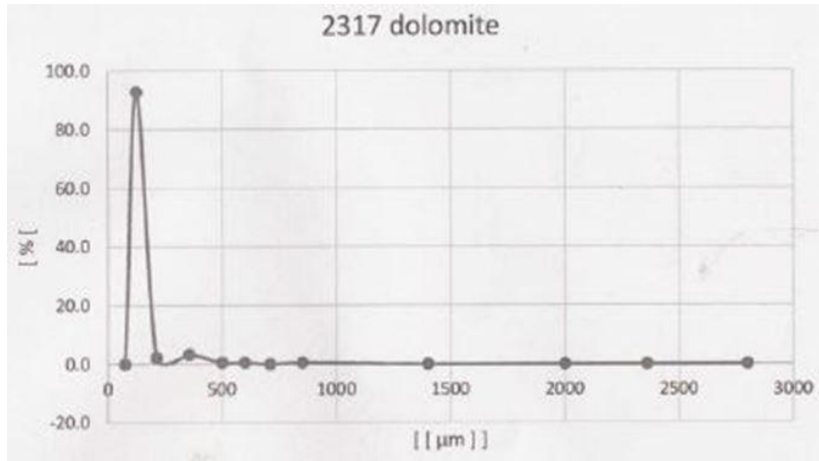


Figure 15: Particles size distribution, (Drytech Int.).

cript

Lime Cake Pressure Resistance

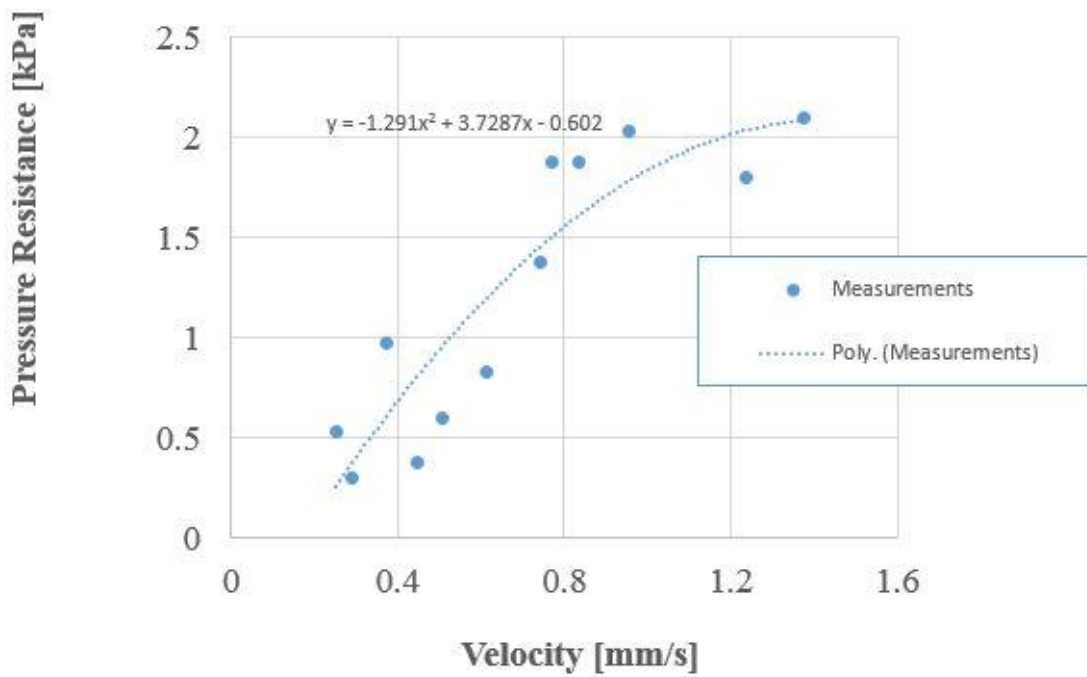


Figure 16: Pressure drops variation across the filtration cake

The Dupuit-Forchheimer model [6], as illustrated in Equation 2, can be used as the foundational model for the analytical representation of experimental measurements:

$$-\nabla p = \frac{\mu}{k_p} v + \beta \rho v^2 \quad \text{eq. 2}$$

However, in this study we employed the Ergun empirical model, as a derivation of the Dupuit-Forchheimer approximation:

$$-\frac{dp}{L} = \frac{150\mu(1-\chi)^2v}{\chi^3D_p^2} + \frac{1.75\rho(1-\chi)v^2}{\chi^3D_p} \quad \text{eq. 3}$$

where: dp is the pressure drop across the cake (Pa), μ is the fluid dynamic viscosity (1.1E-4kg/ms), ρ is the fluid density (1000kg/m³), D_p is the diameter of particles [100 μ m], shown in Figure 15, χ is the volume porosity (dimensionless), L is the filtration cake thickness (0.023m) and v is the fluid specific velocity in range from 0.003 m/s to 0.015m/s. The wet and dry cake porosity was experimentally measured to be 0.37 and 0.5 respectively.

Comparing Equation 2 and Equation 3 gives the final viscous P_v and internal P_i terms as:

$$P_v = \frac{150\mu(1-\chi)^2}{\chi^3D_p^2} \quad \text{eq. 4}$$

and

$$P_i = \frac{1.75\rho(1-\chi)}{\chi^3D_p} \quad \text{eq. 5}$$

The values of calculated P_v and P_i terms are 3.3E+7 and 7.0E+7 respectively.

In experiment the pressure drop varies between 0.3kPa and 2.1kPa across the cake, as shown in Figure 16.

Applying P_v and P_i terms the pressure filtration cake resistance for a velocity $v=0.0016$ m/s was calculated to be 2.5 kPa, which is in line with the experimental measurements, shown in Figure 16. The terms P_v and P_i are used in the final assembly model.

Filter's Disc Sector Numerical Analysis

For the purposes of this investigation, only one sector of the disc was modelled employing CFD (ccm+) techniques in a scale 1:1. This is shown in Figure 17(a). The filter has 10 discs and each disc has 24 sectors. During operation, only 6 sectors are submerged in the slurry at a time. Figure 17(b) shows the domain discretisation applied to the sector.

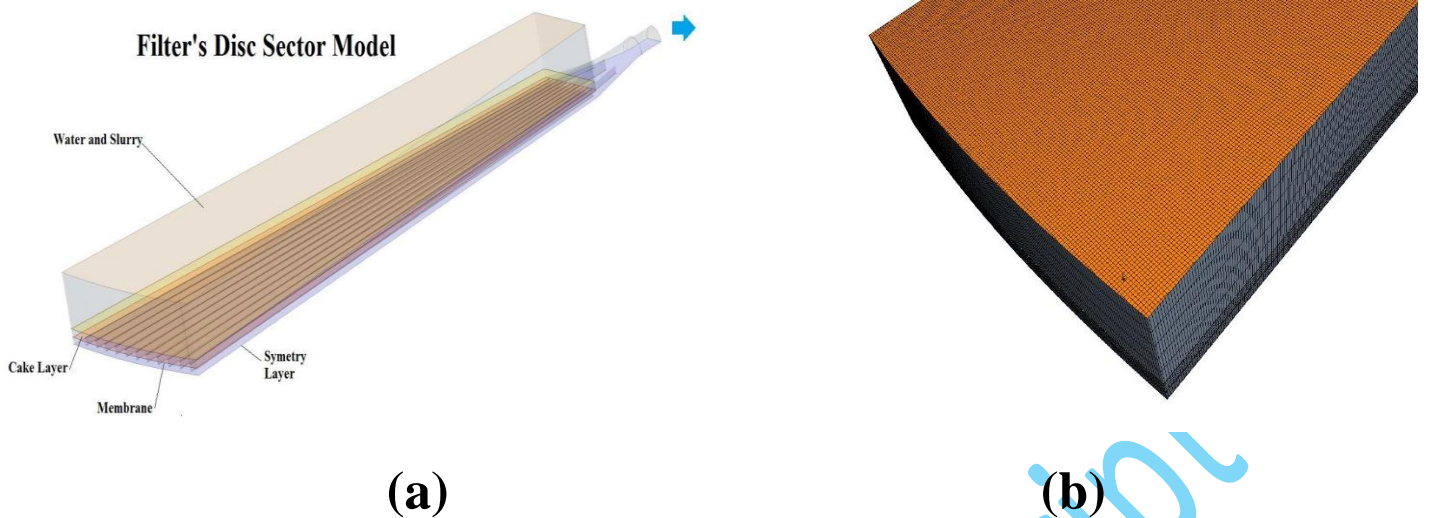


Figure 17: Sector model geometry a) Plain, b) Meshed

A base hexahedral cell with a size of 0.003m was used and a total of approximately 4 million cells were modelled after a mesh sensitivity study. The model was set up as a steady state, segregated flow, with a constant density, realisable k- ϵ and all wall y+ treatment. The membrane was defined as a perforated baffle with viscous coefficient P_v , as calculated in section (Testing Composition Pressure Drop). To simulate the filtrate cake layer resistance the viscous P_v and internal P_i terms calculated in section, Filtrate Cake Pressure Dop Experiment, were used.

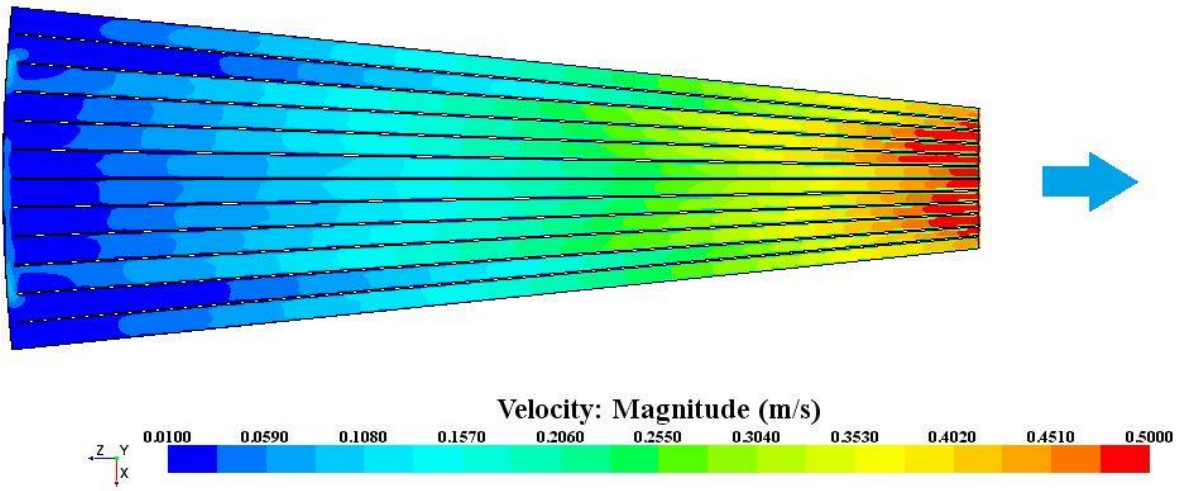
To save the computational power, the model was configured as a symmetric model with the symmetry plane at the sector's horizontal centre line. The average mass flow rate was set to 1.0 kg/s $= \frac{450 \times 1000}{3600 \times 60 \times 2}$ at the outlet boundary condition. The inlet boundary was set up at the top of filtration cake layer.

Simulation Results

Figure 18 a) shows the profile of velocities at the membrane. These velocities across the membrane range between 0.01 and 0.42 m/s for a porosity of 0.5. The maximum velocity of 0.5 m/s was recorded towards the outlet at the barrel end of the sector. The regions of high velocity on the membrane correspond to regions that exhibited a high failure rate in service. Figure 18 b) shows the velocity profiles at the centre of the sector (symmetry plane).

The velocity values at the membrane and centre of sector differ significantly. Velocities at the membrane are higher than at the centre. They are "inside" the membrane velocities, where the cross area of the flow is lower due to membrane porosity. However, the velocity pattern still stays the same.

a)



b)

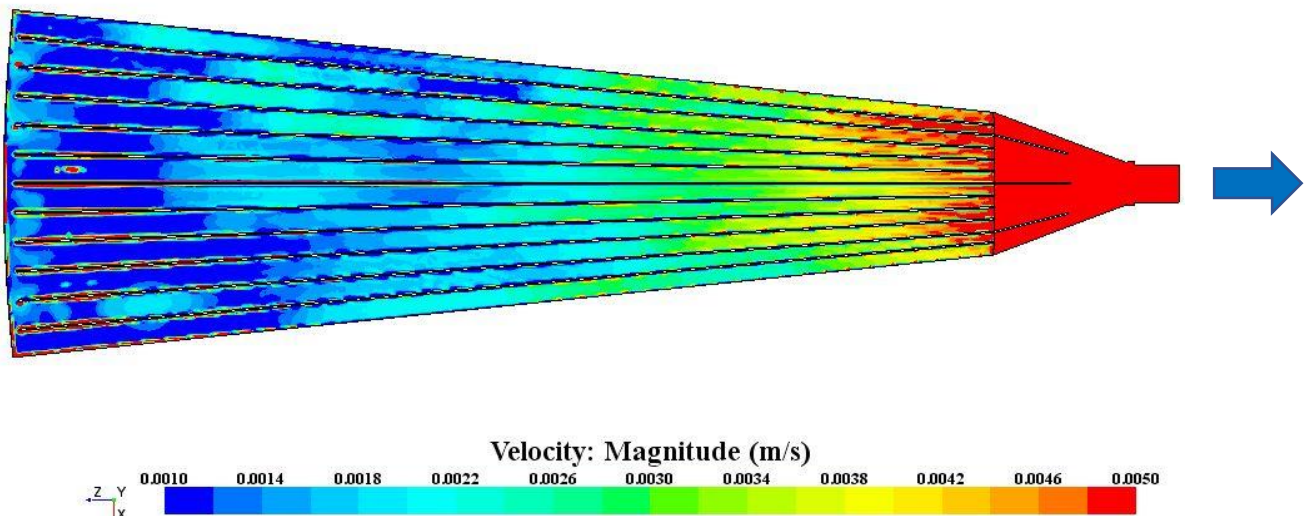


Figure 18: Flow velocity profiles: (a) At the membrane (b) At centre of sector (symmetry plane)

The pressure resistance variation at the membrane of the sector is shown in Figure 19. The calculated max suction pressure was approximately -2.6 kPa. The average pressure resistance through the membrane was calculated to be 2.07kPa, shown in Figure 11. The average pressure resistance through the cake was 1.2 kPa, shown in Figure 16. Setting up the pressure 0.0 kPa at the cake top layer, the total average pressure resistance was approximately 3.27 kPa = (2.07+1.2) kPa, which is comparable with model calculated average pressure resistance 2.25 kPa, illustrated in Figure 19. These observations are in line with outcome of 0.04 bar depicted on Figure 6.

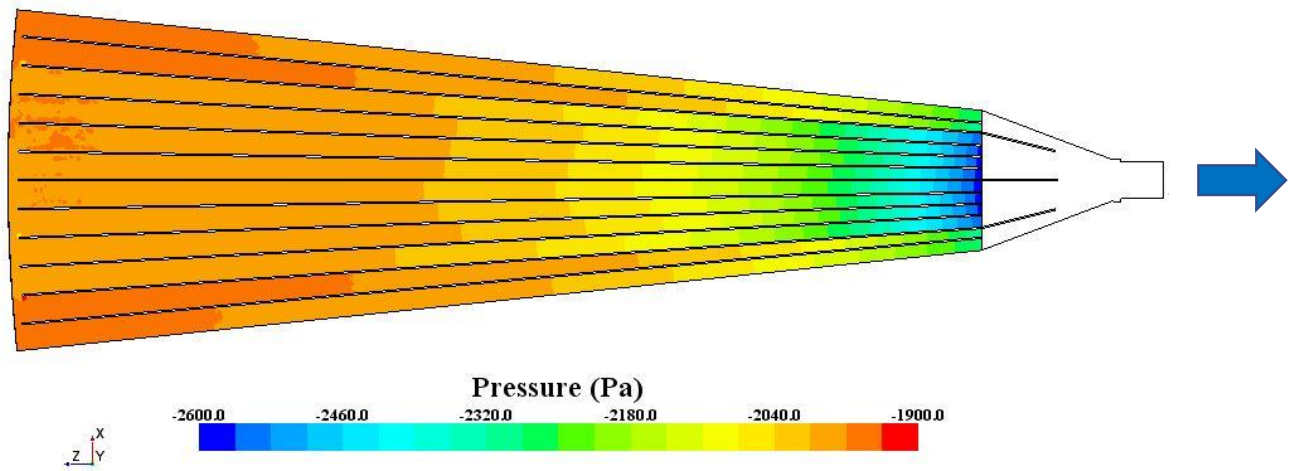


Figure 19: Pressure distribution at the centre of the sector (symmetry plane)

Conclusions

A fit-for-purpose CFD model was successfully validated and used to study the performance parameters of an in-service rotary drum vacuum dryer. A parametric study of the system revealed that the filter membrane was the kernel factor responsible for the development of flow pressure resistance. Additionally, the velocities and porosity also had an effect on the pressure resistance of the entire system. It was however concluded that the pressure was not harmful to filtration membrane. The fluid and hence fluid velocities reaching 0.5m/s in the sector top area close to the sector outlet had the most detrimental effect on the filtration membrane leading to the severe wear and ultimately to its breakage, as recorded on the backing plate holes

It is evident that the highest likelihood of damage to the membrane occurs when velocity of filtration water reaches the highest level. The highest velocity, as illustrated in Figure 6, is when the filtration cake is removed and consequently cake suction pressure is at the lowest level.

The membrane damage problem arose from the mistaken geometrical design of the filtration disc (sectors).

Acknowledgment

The authors would like to acknowledge the technical and testing support provided by Drytech International (Pty) Ltd company especially the design and construction of the test rigs.

References

- [1] T. Sivakumar, G. Vijayaraghavan and A. Vimal Kumar, "Enhancing the Performance of Rotary Vacuum Drum Filter," *International Journal of Advanced Engineering Technology*, vol. II, no. IV, pp. 41-47, 2011.
- [2] H. Theliander, "On the Filtration Properties of Lime Mud," *Nordic Pulp and Paper Research Journal*, vol. 5, no. 2, pp. 74-82, 1990.
- [3] T. D. Davis and R. A. Caretta, "Analysis of a Continuous Rotary-drum Filtration System," *AIChE Journal*, vol. 56, no. 7, pp. 1737-1738, 2010.
- [4] B. A. Wills and J. A. Finch, *Wills' Mineral Processing Technology: An Introduction to the Practical Aspects of Ore Treatment and Mineral Recovery*, Oxford: Butterworth-Heinemann, 2016.
- [5] C. J. Geankoplis, A. A. Hersel and D. H. Lepek, *Transport Processes and Separation Process Principles*, Boston: Prentice Hall, 2018.
- [6] J. Petrasch, F. Meier, H. Friess and A. Steinfeld, "Tomography Based Determination of Permeability, Dupuit-Forchheimer Coefficient, and Interfacial Heat Transfer Coefficient in Reticulate Porous Ceramics," *International Journal of Heat and Fluid Flow*, vol. 29, pp. 315-326, 2008.